Egypt. J. Chem. **Vol. 65,** No. 1 pp. 245 - 257 (2022)

Egyptian Journal of Chemistry

http://ejchem.journals.ekb.eg/

Synthesis, Characterizations, DFT, and Antibacterial Evaluation of Some Complexes of Co (II), Ni(II), Cu(II), Zn (II), and Cd (II) with Schiff Ligand

Sahbaa Ali Ahmed, Saba Mumtaz Salih, and Esraa Ali Hasan

Chemistry Department, College of Science, University of Mosul., Iraq

Abstract

New metal complexes of tridentate N2O Schiff bases were synthesized via reaction of pyrazole Schiff base and metal chloride ions of cobalt, Nickel, copper, Zinc, and cadmium in absolutye ethanol at reflux temperatures. New complexes were characterized according to their elemental analyses, Nuclear magnetic resonance of hydrogen proton (H NMR), ultraviolet visible spectra (UV-vis), and X-ray diffraction (XRD), together with thermal analyses such as TG, DTA, DSC and Density Functional Theory (DFT). Also, antimicrobial activity of new metal complexes was studied and evaluated against a panel of one positive Gram bacteria (*Staphylococcus aureus*) and two negative Gram bacteria (*Escherichia coli, and Pseudomonas aereuginosa*).

Keywords: Schiff base, Serine, Metal complexes, Antimicrobial activity.

Introduction

Pyrazole is a heterocyclic moiety that has five member ring with two nitrogen atoms and three carbons. Pyrazole and its derivatives have potential activity as pharmaceutical, medicinal and biological activities. These activities are a wide such as antimicrobial[1], anticonvulsant[2], anticancer[1, 3] anti-inflammatory[4], antidepressant [5] and antitumor [6] together with antipyretic and analgesic properties[7, 8]. Also, pyrazole has enzymatic activity as inhibitory activity against enzymes[9]. Schiff base is a technique that applied on compounds that used as a ligand in formation of metal complexes and they were synthesized via reaction of carbonyl compounds with amine compounds. Schiff bases has a wide variety of biological activities such as antimicrobial, [10] antitumor [11]anti-inflammatory with pharmacological activity[12].

In the same manner, antipyrine is considered one of the valuable discovery in the field of medicinal and organic chemistry because of its activity of such antipyretic, less toxic, nonpaid analgesic, anti-inflammatory drug together with its metabolism by liver to exert via urine [13]. Beside, Schiff bases of antipyrine derivatives have an important roles in coordination chemistry[14].

Metal complexes is a mixture between metal and organic compounds named ligand which in general is a Schiff base of carbonyl compounds that condensed with primary amines. Metal ions are used in many drugs such as cisplatin which is one of the leading metal ions [15].

According to above survey and in continuation of our work in organic synthesis, we aim to synthesize a new series of metal complexes to study their characterization, Density Functional Theory (DFT) and antimicrobial activity.

Results and Discussion

First, we synthesized Schiff base derivative **3** in a good yield via reaction of aminoantipyrine **1** with benzaldehyde derivative **2** in absolute ethanol at reflux temperature for three hours according to literature

*Corresponding author e-mail: sahbaa-ali@uomosul.edu.iq.; (Sahbaa Ali Ahmed).
Receive Date: 11 June 2021, Revise Date: 08 July 2021, Accept Date: 10 July 2021
DOI: 10.21608/EJCHEM.2021.80166.3963

methods [16, 17](Scheme 1). The obtained Schiff base namely 4-((4-hydroxy-2-methoxybenzylidene)amino)-1,5-dimethyl-2-phenyl-1,2-dihydro-3H-pyrazol-3-one (**3**) is elucidated on the bases of H NMR, IR and mass spectrum.

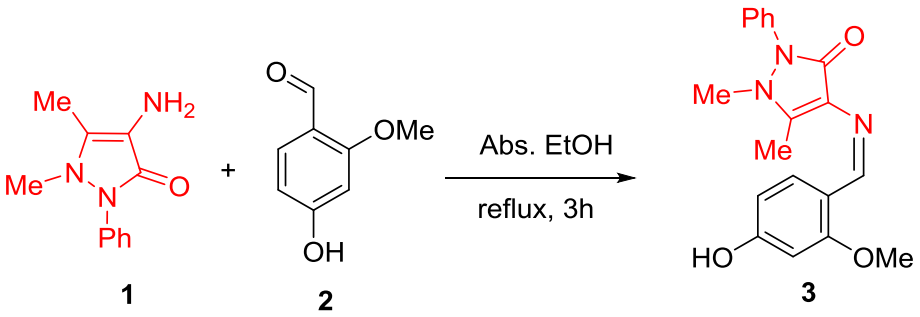

Scheme 1: Schiff base synthesis

On the other hand, a condensation between potassium L-serinate (**4**) and Schiff base 3 is done in absolute ethanol at reflux temperature to afford Schiff base ligand (**5**) in a high yield (Scheme 2). Novel ligand was characterized on its elemental analyses and spectroscopic data to afford potassium(S)-3-hydroxy -2-(((E) -4-(((Z) -4-hydroxy-2-methoxy-benzylidene) amino)-1,5-dimethy l-2-phenyl-1,2-dihydro-3H –pyrazol -3-ylidene) amino)propanoate (**5**).

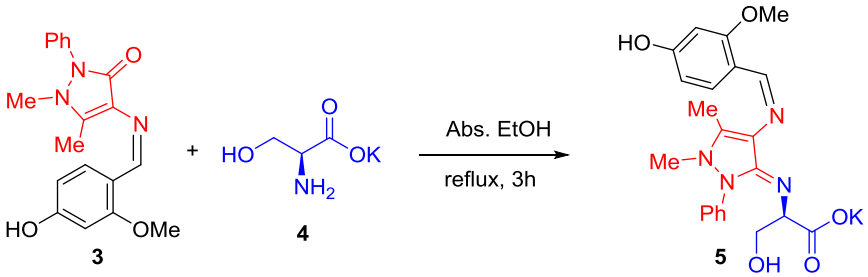

Scheme 2: Schiff base ligand (5) synthesis

Reaction of Schiff base ligand (**5**) with metal (II) chlorides of cobalt, nickel, copper, zinc and cadmium has been analyzed in absolute ethanol at reflux temperature to get metal complexes 6a-e in an excellent yield (Scheme 3).

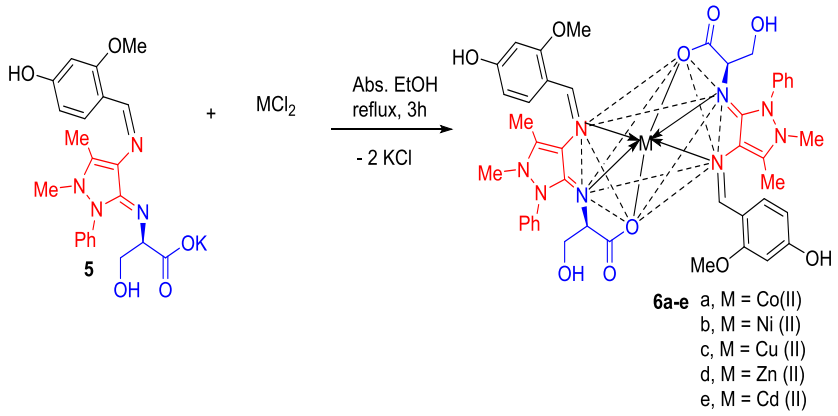

Scheme 3: Metal complexes synthesis

Physical and elemental analyses characterization

Table 1 has a detailed physical properties of ligand **5** and complexes **6a-e** to have a little bit structure form of these compounds. Also, molar conductivity was measured and calculated after dissolving in DMF at room temperature to confirm non-electrolytic nature of complexes with their lower conductance value 9.2–14.7ohm $^{-1}$cm^{2}mole^{-1} (Table 2).

These obtained data is reasonable with striped sized molecular procedures of ligand **5** and complexes **6a-e** in accordance of obtained spectra data to magnetic capability and molar conductivity of complexes to afford that every complex has ratio 1:2 [M:L] to act as tridentate ligand (Table 2).

IR spectra

IR spectra of ligand **5** and its complexes **6a-e** is cited at table 3, comparison between IR spectrum of Ligand **5** and complexes revealed presence of C=N peak at 1677cm^{-1} which converted low frequency at 1641-1648cm^{-1} in all metal complexes which revealed sharing of nitrogen atom of C=N bond in coordination with metal ions. This coordination reduces azomethine electron density as it is cleared in νassym (COO^-) of ligand **5** at 1582cm^{-1} which highly shifted to 1590-1595cm^{-1} in complexes. Also, νsym (COO^-) of ligand **5** was observed t 1490cm^{-1} and shifted to 1450-1459cm^{-1} in complexes **6a-e** indicating that carboxylic group is linked to metal ion via oxygen atom. Metal oxygen bond (M-O) appeared at 515–550 cm^{-1} and (M-N) at 404–448 cm^{-1} as medium bands. IR spectrum of ligand **5** and complex **6a**, complex **6c** had been shown in Figures 1-3.

Nuclear Magnetic Resonance

NMR of ligand showed signals at δ 9.60 ppm as singlet proton of OH group, δ 9.32 ppm of azomethine proton (H-C=N-), δ 7.81–6.04ppm as multiplet 8H, of aromatic protons, 3.81 as triplet signal of -CH_2OH of amino acid, δ 3.70ppm of methoxy protons, δ 2.52 ppm of methyl group, and at δ 2.44ppm as triplet signal of methane proton CH-COO (Figure 4).

Table. 1. Elemental analyses and physical properties of ligand (5) and complexes (6a-e)

Compound	Colour	m.p. ºC	Yield %	M. Formula (MWt)	Found (calc)%			
					C	H	N	M
5	Light yellow	190	82	$C_{22}H_{23}KN_4O_5$ (462.13)	57.13 (57.08)	5.01 (5.05)	12.11 (12.15)	--
6a	Light Green	215	71	$C_{44}H_{46}N_8O_{10}Co$ (905.27)	58.34 (58.46)	5.12 (5.16)	12.37 (12.41)	6.51 (6.58)
6b	Green	224	80	$C_{44}H_{46}N_8O_{10}Ni$ (905.59)	58.36 (58.43)	5.12 (5.15)	11.37 (11.40)	6.48 (6.55)
6c	Dark brown	222	79	$C_{44}H_{46}N_8O_{10}Cu$ (909.26)	58.05 (58.10)	5.09 (5.15)	12.31 (12.40)	6.98 (7.02)
6d	Dark yellow	226	75	$C_{44}H_{46}N_8O_{10}Zn$ (912.28)	57.93 (57.98)	5.08 (5.02)	12.28 (12.30)	7.17 (7.25)
6e	Lemon yellow	229	84	$C_{44}H_{46}N_8O_{10}Cd$ (960.24)	55.09 (55.10)	4.83 (4.90)	11.68 (11.71)	11.72 (11.80)

Table 2: The electronic spectra, magnetic susceptibility and molar conductance values

Compound	Band position, cm^{-1}	Transition	$\Omega^{-1}cm^2mol^{-1}$	Geometry (Suggested)	μeff (B.M.)
5	36485	π→ π*	--	--	--
	23202	n→π*			
6a	39063	Centre ligand	9.2		
	33670	Centre ligand			
	12987	$^4T_1g(F)\rightarrow{}^4T_2g(F)$			4.71
	16393	$^4T_1g(F)\rightarrow{}^4A_2g(F)$			

	22727	$^4T_1g(F) \rightarrow {}^4T_2g(P)$			
6b	13157 16528 23255	$^3A_2g(F) \rightarrow {}^3T_2g(F)$ $^3A_2g(F) \rightarrow {}^3T_1g(F)$ $^3A_2g(F) \rightarrow {}^3T_1g(P)$	14.7	Octahedral	3.19
6c	15650	$^2Eg \rightarrow {}^2T_2g$	13.2	Octahedral	1.73
6d	25877	d $\pi(Zn)^{+2} \rightarrow \pi^*(L)$	9.5	Octahedral	Dia
6e	21128	d $\pi(Cd)^{+2} \rightarrow \pi^*(L)$	11.8	Octahedral	Dia

b

Table 3: IR of ligand 5 and complexes 6a-e

Compound	ν (C = N)	ν_{asmmy} (COO^-)	ν_{smmy} (COO^-)	ν (M–N)	ν (M–O)
5	1677	1582	1490	----	----
6a	1641	1595	1450	431	546
6b	1644	1591	1456	432	550
6c	1641	1595	1450	404	515
6d	1647	1592	1459	447	547
6e	1648	1590	1459	448	550

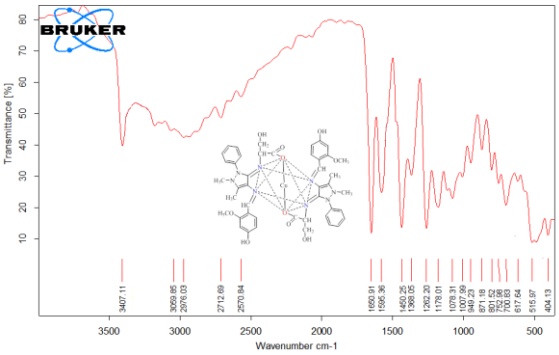

Figure 1: IR spectrum of ligand 5

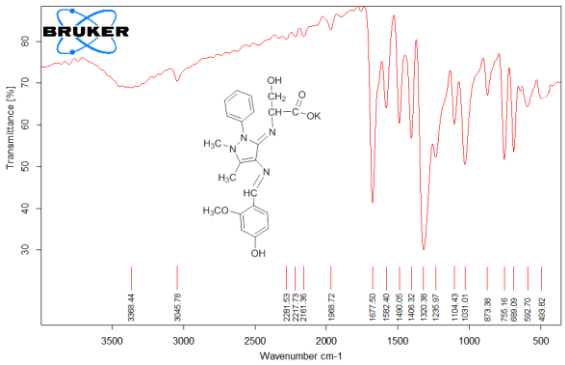

Figure 3: IR spectrum of complex 6c

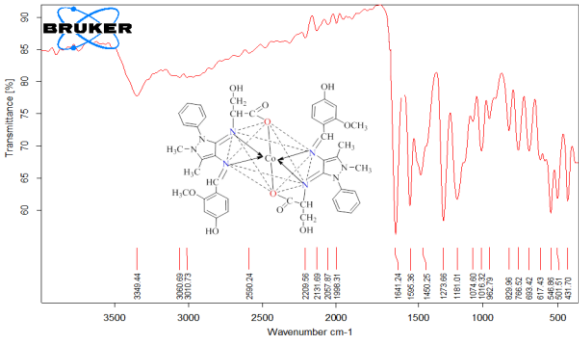

Figure 2: IR spectrum of complex 6a

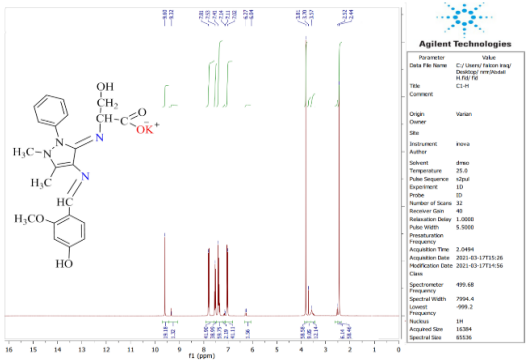

Figure 4: H NMR of ligand 5

Electronic Spectra and magnetic moments

Magnetic moments and electronic spectra measurements are used to determine geometric structures ligand **5** and complexes **6a-e** (Table 3). Ligand electronic spectrum revealed absorption bands at 36485 cm^{-1} , 23202 cm^{-1} corresponding to $\pi \rightarrow \pi^*$ and $n \rightarrow \pi^*$, Complex **6a** electronic spectrum showed weak bands at 12987, 16393 and 22727 cm^{-1} which related to octahedral geometry corresponding to $^4T_1g(F) \rightarrow {}^4T_2g(F)(\nu_1)$, $^4T_1g(F) \rightarrow {}^4A_2g(F)(\nu_2)$, $^4T_1g(F) \rightarrow {}^4T_2g(P)(\nu_3)$ transitions respectively[18, 19]. Also, complex **6a** supported octahedral geometry via its magnetic moment of value 4.71B.M. Complex **6b** has three weak bands at 13157,16528 and 23255 cm^{-1} that related to $^3A_2g(F) \rightarrow {}^3T_2g(F)$, $^3A_2g\ (F) \rightarrow {}^3T_1g\ (F)$, $^3A_2g(F) \rightarrow {}^3T_1g(P)$[20]. which are characteristic of octahedral geometry[23]the magnetic moment of the Ni(II) complex which is found to be 3.19 B.M. also supports octahedral geometry for the complex. Complex **6c** depicts a broad band with maximum at 15650 cm^{-1} assignable to $^2Eg \rightarrow {}^2T_2g$, with band broadness due to octahedral geometry, shows magnetic moment of value 1.73 B.M. predicted for one unpaired electron, monomeric, and consistent with a distorted octahedral geometry [26,27]. Complexes **6d,e** were diamagnetic and have an octahedral geometry according to empirical formula.

X-ray diffraction Analysis

X-ray diffraction, of the ligand **5** and complex **6e** showed diffraction peaks at 2θ=10-60 to indicate that ligand and complex are crystalline mixture with amorphous phase (figure 5). Using equation of Bragg "ny = 2d sin θ" to calculate reflection d spacing value, and Scherer equation "D=K λ /β cos θ" to calculate average of particle size. The crystallite size of the complex is 35.0–39.90 nm the values in Table (4). Whole of the peaks calculated from observed inter-planar distance values were compared to the one that was reported. All significant peaks unit cell calculations for hexagonal symmetry were reported. These findings are agreement with the XRD peaks of other Cd(II) complexes mentioned in literature

.

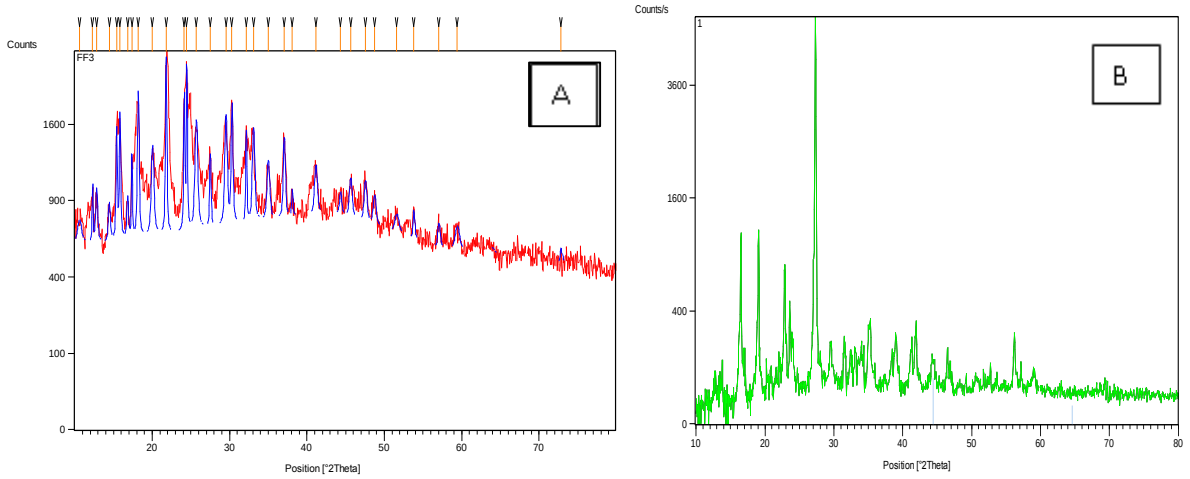

Figure 5: X-ray diffraction patterns for (A): Ligand,(B): Cd(II).

Table.4.Inter planar distances 2θ, and FWHM relative intensity for complex 6e.

Peak no. (Strongest)	2θ(deg.)	Height [cts.]	FWHM [°2Th.]	d(Å)	Intensity (counts)
2	18.1934	1211.45	0.2460	4.87624	74.06
6	21.7985	1622.45	0.1968	4.07725	99.19
7	24.4639	1635.70	0.1476	3.63873	100.00
9	25.6939	868.96	0.3936	3.46726	53.12
10	29.5243	902.18	0.3444	3.02557	55.16
12	30.3032	1047.48	0.2460	2.94956	64.04

Thermo gravimetric analysis

Ligand **5** and complexes **6a-e** had been registered in range between 25-800 ºC with TG-DTA values (Table 5). This temperature range 25–800°C causes decomposition with a mass loss of 1.5-3% at about 28-215°C due to loss of CO_2 evolution and moisture[20, 21]. Mass lose is about 9.3-22.6 % between 115-320°C as a result of loss of coordinated water with methyl group of ligand. Also, at range 150-275°C, the compound lost 19.5-33.1% as result of azomethine group and at range 150-456°C mass loss is 67.7-80.1% as result of pyrazole ring loss which is also supported by an exothermic peaks at 600 700°C as residual mass of 88% with the formalization of CoO, NiO , and CdO (Table 5).

Table.5. DTG, T.G and DSC of ligand 5 and complexes 6a-e

Compounds	TG Range (°C	DTG Max (°C)	Mass loss%	Assignment	Residue	DSC (°C)
5	28-150	296	1.55	Evolution of CO_2 and moisture	--	230(+)
	150-275	425	10.14	Loss Me		
	275-345		26.50	Loss C=N-		418 (+)
	345-420		35.88	Loss pyrazole ring		
	420-545		74.1	A part of the Ligand		
	545-800		81.9			
6a	30-125	155	1.56	Evolution of CO_2 and moisture		250 (+)
	125-175	260	9.36	Loss Me		
	175-300	375	19.5	Loss C=N-	CoO	370 (+)
	300-455		69.42	Loss pyrazole ring And		
	455-800		88.92	A part of the ligand.		
6b	28-115	235	2.43	Evolution of CO_2 and moisture		385 (+)
	115-265	385	22.68	Loss Me	NiO	405 (+)
	265-325	411	27.54	Loss C=N-		515(+)
	325-490	505	80.19	and Loss pyrazole ring		
	490-800		88.29	A part of the ligand		
6c	30-215	345	3.08	Evolution of CO_2 and moisture		340 (+)
	215-320	415	12.38	Loss Me	CdO	410 (+)
	320-450	465	33.15	Loss C=N-		460(+)
	450-565		67.75	and Loss pyrazole ring		
	565-800		85.40	A part of the Ligand		

Geometry Optimization

We have observed some points after data analysis as the following:

1. After complex formation, coordination bong grew longer with a lot of variance; coordination bond of complexes are Cd(162)-N(131)-C(132) , N(149)-Cd(162)-O(161), N(131)-Cd(162)-O(135), N(149)-Cd(162)-O(161) this indicate that azomethine (-C=N) had been included via protonated O groups and others.
2. Active groups that shared in complexation are longer than of those exist in ligand **5** such as N,N, and O.
3. Cadmium complex central bond angels are within octahedral geometry range. [22, 23] while bond angels around ligand were slightly changed over complexation.
4. Intra-molecular hydrogen bonds are accountable for lowering in H-N angels of azomethine (Figure 6).[23, 24]

Potential Electrostatic in Molecules (MEP)

Molecules Electrostatic potential (MEP) plot depends on constant electron density surface and it used to test the relationship between two major factors physicochemical properties and molecular structures. Also, MEP can be used as grasping interactions of molecular biology and to reactive sites of compounds to deduce electrophilic and nucleophilic chemical reactivity.

There are three colour zones, the negative electrostatic potential that related to MEP was had red colour and electron-poor zone with blue colour for nucleophilic attack, while neutral electrostatic potential is green region. electrophilic reactivity is negative zone linker [24].

Figure 7 showed ligand **5** three dimensional root and compound **6e** in MEP plot. Ligand O,Ns have more negative charge surface to be vulnerable sites of electrophilic attack. Also, Figure 8 support these complexation and it showed that metal core was enclitic by a larger negative charge .

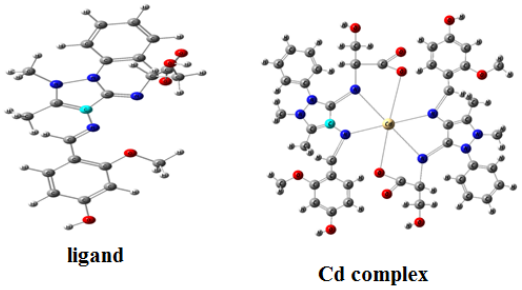

Fig.6. the optimized structure of (a) Ligand and (b) Cd (II)-complex

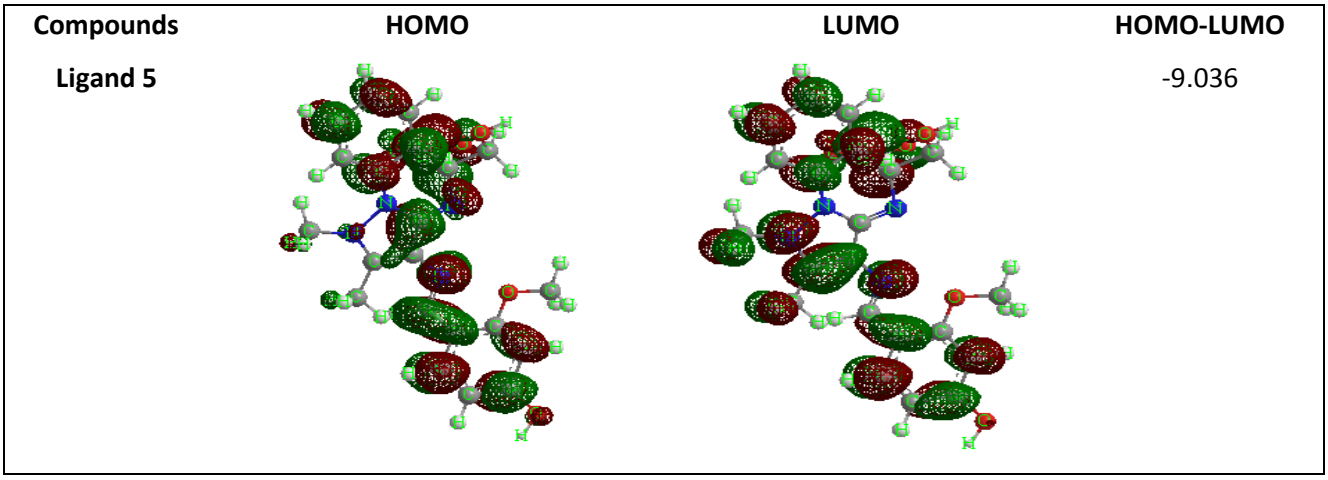

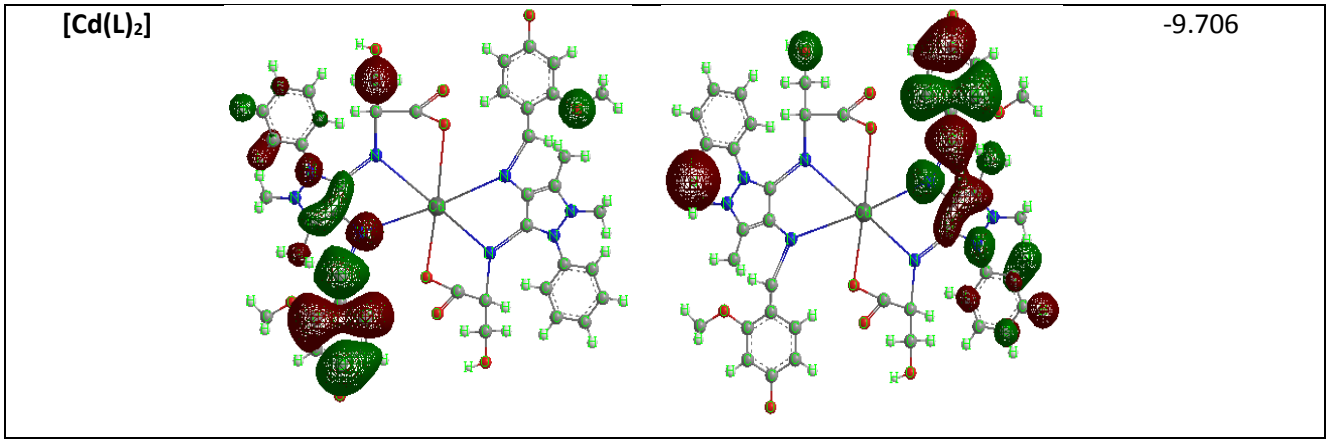

Fig.7. Molecular electrostatic potential map of ligand and cadmium complex

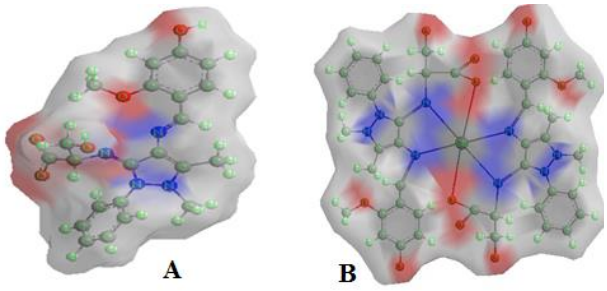

Figure 8: Surface phase of frontier orbitals of ligand 5 and cadmium complex

Molecular Parameters:

As examples of molecular parameters, Ligand **5** and compound **6d** were depicted in figure 7 to show their HOMO, LUMO, and energy band differences, as the key orbitals involved in chemical constancy was LUMO [25-27], while HOMO represented capability of compounds as electron donors and LUMO as electron acceptors.

In another way, HOMO energy is proportional to its size and LUMO energy is directly comparative to electron affinity. So, boundary energies, optical and electric states, are crucial causing disparity in energy between LUMO and HOMO to allow for the computation of electron conductivity.

Furthermore, energy hiatus is used in characterization of spectroscopic characteristics and molecular constancy of molecular systems. As chemically soft polarizable molecule has a smaller energy hiatus. Also, HOMO-LUMO energy gap is used as a method for evaluating chemical reaction and kinetic stability of molecule. i.e. easier exit a molecule means lower the energy gap and higher the energy gap is with higher kinetic stability, lower molecule's chemical reactivity.

Complexation existence at molecular structure depends on modification in ligand **5** energy gap. Accepted electrons higher capability is due to increment of total electrophilicity to indicate that ligand **5** has higher potential for donation, molecular stability and reactivity Also, molecular stability and reactivity can be computed via absolute hardness and smoothness. This can be occurred by comparing measured binding energy of compounds **6a-e** and ligand **5**, these calculations afforded that measured energy value increased in ligand **5** indicated that constancy of complex **6e** was greater than that of ligand **5**.

For Structures confirmation of compounds there are many parameters such as global softness S, electrophilicity index (N), chemical

potentials Pi, global electrophilicity, and extra electronic charge Nmax (Table 6). Ligand **5** and Complex **6e** have a high value likelihood and priority according to the findings, in accordance with experimental evidence. The next equations were utilized to measure the quantum chemical parameters mentioned (Figure 7).

DE = ELUMO - EHOMO .....(1)

$$\chi = \frac{-(E_{HOMO} + E_{LUMO})}{2} \quad \text{------ (2)}$$

$$\eta = \frac{E_{LUMO} - E_{HOMO}}{2} \quad \text{------ (3)}$$

$$\sigma = \frac{1}{\eta'} \quad \text{------ (4)}$$

$$\rho i = -\chi' \quad \text{------ (5)}$$

$$\omega = \frac{Pi^2}{2\eta'} \quad \text{------ (7)}$$

$$S = \frac{1}{2\eta'} \quad \text{------ (6)}$$

$$\Delta N_{max} = \frac{Pi}{\eta'} \quad \text{------ (8)}$$

Table.6.The quantum chemical parameters determined of ligand 5 and Cd(II) complex.

The quantum parameter	Ligand	$[Cd(L)_2]$
E (a.u.)	−1402.10	−1400.98
Dipole moment (Debye)	20.1392	20.1393
EHOMO (eV)	−6.164	−4.950
ELUMO (eV)	−0.607	−2.670
Δ E (eV)	5.557	2.28
`χ(eV)	3.3855	3.8100
η (eV)	2.7785	1.1400
σ $(eV)^{-1}$	0.360	0.8771
Pi (eV)	-3.3855	-3.8100
S $(eV)^{-1}$	2.06255	0.6610
ω (eV)	6.5930	6.3667
ΔN max	1.2184	3.3421

Antibacterial activity

Antibacterial activity of ligand **5** and complexes **6a-e** was investigated against a panel of one positive Gram bacteria (*Staphylococcus aureus*) and two negative Gram bacteria (*Escherichia coli, and Pseudomonas aereuguinosa*) in comparison with Amoxicillin as reference drug (Table 7).

The results revealed that all compound that synthesized are active against Gram bacteria using disc diffusion method with medium of nutrients agar with replication of experiments three times. Also, metal complexes **6a-e** showed higher activity than ligand **5** which may be as a result of ligand orbitals overlap (Chelation theory)[28] . Also, metal polarity decreased to lower degree during chelation,

delocalization of π -electrons over the entire chelate ring and increases the complexes lipophilicity which causes break down of cell's permeability; slowing down normal cell processes shown in Figure 9.

.

Table 7: Minimum Inhibitory Concentration of ligand 5 and complexes 6a-e against growth of bacteria (Mg/ml).

Compound	*Escherichia coli*	*Staphylococcus aureus*	*Pseudomonas aereuginosa*
5	12	10	8
6a	19	18	16
6b	28	28	24
6c	24	28	25
6d	20	24	20
Amoxicillin	**8.9**	**11**	**9**

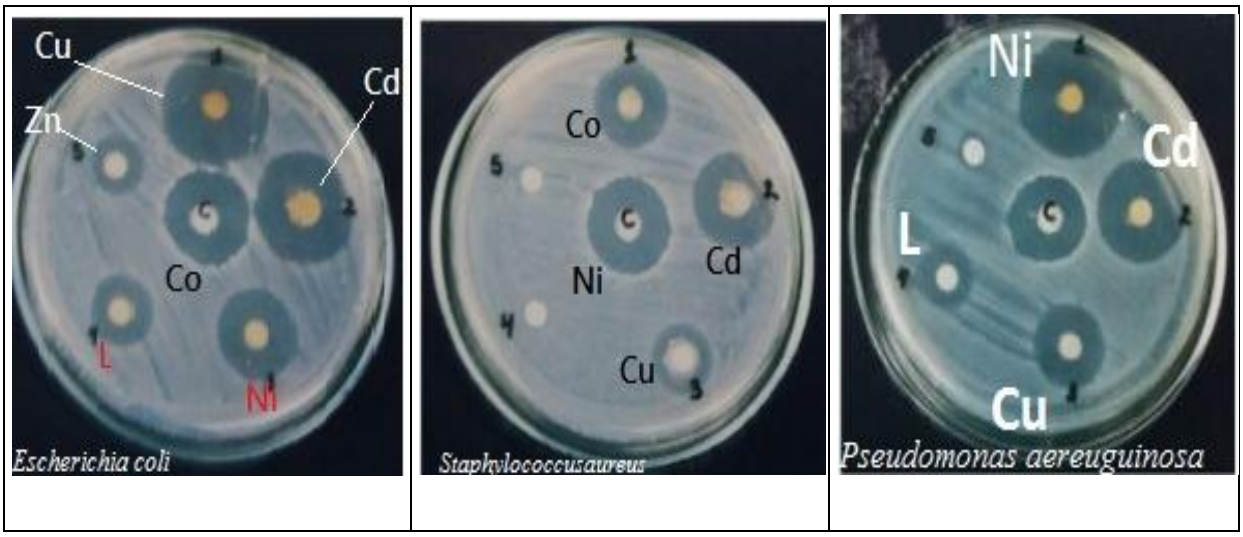

Figure 9: antibacterial screening results

.**Experimental**

All chemical that used in reactions are purchased from known chemical companies and it used without purification. Melting point were measured on electro-thermal apparatus 9300 and uncorrected. Elemental analyses were recorded on perkinelmer USA-2400-II . molar conductivity is measured in DMF model Eutech-pc700. UV spectra were recorded on Shimadzu spectrophotometer 1700UV. IR spectra were measured on Shimadzu FTIR. NMR were recorded on Bruker 400Hz with internal TMS and DMSO as solvent. Magnetic susceptibility were performed at rt using Guoy's balance. Compounds thermo-gravimetery (DTA, TGA, and DSC) were studied in static form using DuPONT600ATG thermo balance with rheumatic TGA-1000. XRD of complexes is collecting using X'pertpro diffract-meter.

1. Schiff base Synthesis

A mixture of 4-aminoantipyrine (4.06g, 0.02 mol) in 10ml ethanol and 4-hydroxy-2-methoxybenzaldehyde (3.04g ,0.02mol) in 10ml of ethanol was reflex for 3h. After reaction completion (TLC), cooled, to get precipitate, filter, dried and recrystallized (EtOH) to afford yellow crystals of Schiff base **3** [29, 30].

2. Schiff base ligand synthesis

Potassium L-serinate (**4**) [29] in 40mL H_2O:EtOH (1:1, v:v) was added to hot ethanolic potassium

hydroxide (30mL) until homogeneity. This mixture added drop-wise to Schiff base **3** (3.37g, 0.01mol) then reflux for 3h to afford the ligand, dried, recrystallized from ethanol and kept over $CaCl_2$.

3. Synthesis of metal complexes 6a-e

Complexes are synthesized (20 mL) of Schiff base (**5**) (1.85g , 2mmol) ligand was used to alcoholic solution (15mL) of (0.47g , 1mmol), $CoCl_2.6H_2O$ /(0.47g , 1mmol) of $NiCl_2.6H_2O$ / (0.34g , 1mmol) of $CuCl_2.4H_2O$ / (0.48g , 1mmol) of $ZnCl_2.6H_2O$, and (0.59g , 1mmol) of $CdCl_2.6H_2O$ refluxed for 2 h, it was filtered off, washed and dried under vacuum to yield complexes.

Conclusion

From pervious results, we can conclude that Schiff base of aminoantipyrine moiety is easy in synthesis and to deliver it as ligand with potassium serinate. Then this ligand is subjected to metal complexes 6a-e in an excellent yield with metal ions of cobalt, nickel, copper, zinc and cadmium in a ration [2:1, L:M] as tridentate ligand. Their structures were confirmed through different spectroscopic and elemental analyses with thermal gravity analyses to prove these structures as octahedral geometry as a results of coordination of oxygen metal connection. Also, antibacterial activity was tested against three strains of Gram bacteria.

Acknowledgement

Authors thank chemistry department, Science College, University of Mosul for financial support during this work.

References

[1] A. Beheshti, M. Bahrani-Pour, M. Kolahi, E. Shakerzadeh, H. Motamedi, P. Mayer, Synthesis, structural characterization, and density functional theory calculations of the two new Zn (II) complexes as antibacterial and anticancer agents with a neutral flexible tetradentate pyrazole-based ligand, Applied Organometallic Chemistry, 35 (2021) e6173.

[2] M. Abdel-Aziz, G.E.-D.A. Abuo-Rahma, A.A. Hassan, Synthesis of novel pyrazole derivatives and evaluation of their antidepressant and anticonvulsant activities, European journal of medicinal chemistry, 44 (2009) 3480-3487.

[3] I. Bouabdallah, L.A. M'Barek, A. Zyad, A. Ramdani, I. Zidane, A. Melhaoui, Anticancer effect of three pyrazole derivatives, Natural product research, 20 (2006) 1024-1030.

[4] J.-J. Liu, M.-y. Zhao, X. Zhang, X. Zhao, H.-L. Zhu, Pyrazole derivatives as antitumor, anti-inflammatory and antibacterial agents, Mini reviews in medicinal chemistry, 13 (2013) 1957-1966.

[5] A. Alaghaz, S. Alturiqi, R. Ammar, M. Zayed, Synthesis, spectral characterization, docking analysis, DNA binding/cleavage, antimicrobial and cytotoxic activity of new dimeric antipyrine-Schiff base metal complexes, Asian J. Chem., 31 (2019) 199-212.

[6] G.M. Nitulescu, C. Draghici, O.T. Olaru, New potential antitumor pyrazole derivatives: Synthesis and cytotoxic evaluation, International journal of molecular sciences, 14 (2013) 21805-21818.

[7] A.A. Bekhit, S.N. Nasrall, E.J. El-Agroudy, N. Hamouda, A. Abd El-Fattah, S.A. Bekhit, K. Amagase, T.M. Ibrahim, Investigation of the anti-inflammatory and analgesic activities of promising pyrazole derivative, European Journal of Pharmaceutical Sciences, (2021) 106080.

[8] L.C. Ekowo, S.I. Eze, J.C. Ezeorah, T. Groutso, S. Atiga, J.R. Lane, S. Okafor, K.G. Akpomie, O.C. Okparaeke, Synthesis, structure, Hirshfeld surface, DFT and in silico studies of 4-[(E)-(2, 5-dimethoxybenzylidene) amino]-1, 5-dimethyl-2-phenyl-1, 2-dihydro-3H-pyrazol-3-one (DMAP) and its metal complexes, Journal of Molecular Structure, 1210 (2020) 127994.

[9] H.M.Y. Al-Labban, H.M. Sadiq, A.A.J. Aljanaby, Synthesis, Characterization and study biological

activity of some Schiff bases derivatives from 4-amino antipyrine as a starting material, in: Journal of Physics: Conference Series, IOP Publishing, 2019, pp. 052007.

[10] E. Yousif, A. Majeed, K. Al-Sammarrae, N. Salih, J. Salimon, B. Abdullah, Metal complexes of Schiff base: preparation, characterization and antibacterial activity, Arabian Journal of Chemistry, 10 (2017) S1639-S1644.

[11] K. Venkateswarlu, N. Ganji, S. Daravath, K. Kanneboina, K. Rangan, Crystal structure, DNA interactions, antioxidant and antitumor activity of thermally stable Cu (II), Ni (II) and Co (III) complexes of an N, O donor Schiff base ligand, Polyhedron, 171 (2019) 86-97.

[12] J. Kumar, A. Rai, V. Raj, A comprehensive review on the pharmacological activity of schiff base containing derivatives, Organic & Medicinal Chemistry International Journal, 1 (2017) 88-102.

[13] K.M. Elattar, A.A. Fadda, Chemistry of antipyrine, Synthetic Communications, 46 (2016) 1567-1594.

[14] G.H. Elgemeie, M.A. Abu-Zaied, S.A. Loutfy, 4-Aminoantipyrine in carbohydrate research: Design, synthesis and anticancer activity of thioglycosides of a novel class of 4-aminoantipyrines and their corresponding pyrazolopyrimidine and pyrazolopyridine thioglycosides, Tetrahedron, 73 (2017) 5853-5861.

[15] C.X. Zhang, S.J. Lippard, New metal complexes as potential therapeutics, Current opinion in chemical biology, 7 (2003) 481-489.

[16] M.S. Alam, D.-U. Lee, Synthesis, Molecular Structure and Antioxidant Activity of (E)-4-[Benzylideneamino]-1,5-dimethyl-2-phenyl-1H-pyrazol-3(2H)-one, a Schiff Base Ligand of 4-Aminoantipyrine, Journal of Chemical Crystallography, 42 (2012) 93-102.

[17] R.M. Issa, A.M. Khedr, H.F. Rizk, UV–vis, IR and 1H NMR spectroscopic studies of some Schiff bases derivatives of 4-aminoantipyrine, Spectrochimica Acta Part A: Molecular and Biomolecular Spectroscopy, 62 (2005) 621-629.

[18] S. Ramalingam, S. Periandy, S. Mohan, Vibrational spectroscopy (FTIR and FTRaman) investigation using ab initio (HF) and DFT (B3LYP and B3PW91) analysis on the structure of 2-amino pyridine, Spectrochimica Acta Part A: Molecular and Biomolecular Spectroscopy, 77 (2010) 73-81.

[19] W.H. Mahmoud, G.G. Mohamed, M.M. El-Dessouky, Coordination modes of bidentate lornoxicam drug with some transition metal ions. Synthesis, characterization and in vitro antimicrobial and antibreastic cancer activity studies, Spectrochimica Acta Part A: Molecular and Biomolecular Spectroscopy, 122 (2014) 598-608.

[20] G.S. Kurdekar, M. Sathisha, S. Budagumpi, N.V. Kulkarni, V.K. Revankar, D. Suresh, 4-Aminoantipyrine-based Schiff-base transition metal complexes as potent anticonvulsant agents, Medicinal Chemistry Research, 21 (2012) 2273-2279.

[21] S. Chaulia, Metal Complexes of Multidentate Azo Dye Ligand Derived From 4-Aminoantipyrine and 2, 4-Dihydroxy Acetophenone; Synthesis, Characterisation, Computational and Biological Study.

[22] R. Takjoo, S.S. Hayatolgheibi, H.A. Rudbari, Preparation, X-ray structure, spectral analysis, DFT calculation and thermal study on palladium (II) coordination compound with Schiff base derived from S-allyldithiocarbazate, Inorganica Chimica Acta, 447 (2016) 52-58.

[23] T. Yousef, O. Alduaij, S.F. Ahmed, G.A. El-Reash, O. El-Gammal, Structural, DFT and

biological studies on Cr (III) complexes of semi and thiosemicarbazide ligands derived from diketo hydrazide, Journal of Molecular Structure, 1125 (2016) 788-799.

[24] S. Basavaraja, D. Balaji, M.D. Bedre, D. Raghunandan, P.P. Swamy, A. Venkataraman, Solvothermal synthesis and characterization of acicular α-Fe 2 O 3 nanoparticles, Bulletin of materials science, 34 (2011) 1313-1317.

[25] S.A. Ahmed, Nano-Schiff base Ligand: Synthesis, Characterization, DFT, and Antibacterial Evaluation of Some Complexes Derived From 4-(-4-methoxybenzylidene) amino)-Antipyrinyl with Glycine amino acid ligand, in: Journal of Physics: Conference Series, IOP Publishing, 2021, pp. 012003.

[26] W.A. Zordok, S.A. Sadeek, Synthesis, thermal analyses, characterization and biological evaluation of new enrofloxacin vanadium (V) solvates (L)(L= An, DMF, Py, Et3N and o-Tol), Journal of Molecular Structure, 1120 (2016) 50-61.

[27] M. Pelczar, E. Chan, N. Krieg, Host-parasite interaction; nonspecific host resistance, Microbiology concepts and applications, 6 (1999) 478-479.

[28] F. Adeowo, B. Honarparvar, A. Skelton, Density functional theory study on the complexation of NOTA as a bifunctional chelator with radiometal ions, The Journal of Physical Chemistry A, 121 (2017) 6054-6062.

[29] N. Raman, R. Jeyamurugan, Synthesis, characterization, and DNA interaction of mononuclear copper (II) and zinc (II) complexes having a hard–soft NS donor ligand, Journal of Coordination Chemistry, 62 (2009) 2375-2387.

[30] N. Raman, R. Jeyamurugan, S. Sudharsan, K. Karuppasamy, L. Mitu, Metal based pharmacologically active agents: synthesis, structural elucidation, DNA interaction, in vitro antimicrobial and in vitro cytotoxic screening of copper (II) and zinc (II) complexes derived from amino acid based pyrazolone derivatives, Arabian Journal of Chemistry, 6 (2013) 235-247.

.